An Acad Bras Cienc (2024) 96(3): e20230570 DOI 10.1590/0001-3765202420230570
Anais da Academia Brasileira de Ciências | *Annals of the Brazilian Academy of Sciences*
Printed ISSN 0001-3765 I Online ISSN 1678-2690
www.scielo.br/aabc | www.fb.com/aabcjournal

ENGINEERING SCIENCES

Parameter Estimation Using the Inverse Problem Method for Simulating Lateral Inflow and Runoff Depth in a small catchment of Amazon

CINDY T. FALCÓN, CLAUDIO JOSÉ C. BLANCO & DIEGO C. ESTUMANO

Abstract The inverse problem method can be applied to determine the properties of hydrological phenomena and estimate the parameters, which cannot be measured directly. This type of inverse focus can facilitate the implementation of the kinematic wave model (direct model-DM), to fill gaps for lateral inflow rate and runoff depth in watersheds. Thus, the goal of the study was the application of the inverse problem method (IP). The lateral inflow rate was generally obtained as a Fourier transform to represent any watersheds. The study was developed using a small catchment in the Amazon where intense rainfall events occur, producing runoff and sediments, which affect rural populations. Lateral inflow rate and runoff depth were derived using precipitation data and parameters estimated through the KINEROS2 (K2)/direct model (DM) model and the ensuing solution methods with MCMC (Markov chains Monte Carlo)/Fourier transform. The developed method was applied to four rainfall-runoff events, leading to a good fit between the observed and predicted data (Nash-Sutcliffe coefficients between 0.76 and 0.85 and RMSE values between 1.80 mm and 6.72 mm).

Key words: Kinematic waves, KINEROS2, Inverse problem, Parameter estimation.

INTRODUCTION

Information related to the hydrology of a region is significant for environmental impact studies, water resource planning, and hydraulic engineering projects. In particular, most studies based on hydrological simulations in the Amazon can provide valuable spatial and temporal estimates of water resources for climate change studies, agribusiness and family agriculture, which encompass social, economic, political, cultural and environmental aspects relevant to sustainability (Costa et al. 2021, da Silva Cruz et al. 2022). Erosion in watersheds is often caused by a lack of management, affecting the environment through soil loss and the transfer of pollutants to rivers and changing water quality (Lagadec et al. 2016). For assessments of soil loss, hydrological models have been employed and are significant tools to understand and represent the dynamics of physical processes in watersheds (Galina et al. 2018). Villarreal et al. (2022) used hydrological modelling to analyze the influence of surface runoff as a function of land cover change due to forest fires. One way to manage hydrological dynamics is through models and geotechnologies. Several authors associate geoprocessing tools with land use and land cover mapping such as SWAT, AGWA, ARCSWAT combined with physical models, such as KINEROS2 (K2) (Goodrich et al. 2012, Abdalla et al. 2022).

There is undeniable concern about how climate change will affect the Amazon and the world in general in the future (Soito & Freitas 2011, Costa et al. 2021). In this context, the aim is to determine the lateral inflow rate and runoff depth in a small catchment in the Amazon where intense rainfall

events occur, producing runoff and sediments, which affect rural populations. This study considered Fourier transform for simulating lateral inflow rate, a term modelled more generally to represent any watershed. This type of inverse focus can be used as an aid to the analysed direct model (DM), which is the classic kinematic wave model, and is obtained through the mass balance equation, considering uncertainties of the parameters in the modelling (Al-Qurashi et al. 2008, Kennedy et al. 2013, Kim et al. 2014). To apply the inverse problems in the representation of the lateral inflow and runoff depth in other basins, it is necessary to estimate parameters with the data that one wants to represent through simulations (Romanov 2009, Toto et al. 2009, Milledge et al. 2012, Kim et al. 2014). For simulation of lateral inflow rate and runoff depth, discretized precipitation data and physical parameters estimated through the KINEROS2 (K2)/direct model (DM) and the solution methods based on MCMC (Markov chain Monte Carlo)/Fourier transform were used.

The solution of the inverse problem leads to the estimation of the so-called observed data (i.e., synthetic observations) associated with the prediction model. Thus, alternative solutions to the problem should be highlighted, which represent the real scenario (Sanso & Guenni 2000). Among these alternatives, Bayesian techniques were applied in the first step of the solution, with MCMC for the first estimation of the lateral inflow rate. In the second step, the lateral inflow rate was modelled through the optimization of the Fourier transform.

KINEROS2 is a physical model for simulating runoff and sediment yield from agricultural and urban watersheds (Woolhiser et al. 1990). In the modelling, the physical phenomena of interception, infiltration, and surface runoff are considered. K2 has already been used to simulate surface runoff in several watersheds, under wet (Smith et al. 1995), arid, and semiarid conditions (Michaud & Sorooshian 1994, Hantush & Kalin 2005, Al-Qurashi et al. 2008, Kennedy et al. 2013, Kim et al. 2014, An et al. 2019, Kautz et al. 2019, Korgaonkar et al. 2020, Harche et al. 2021, Abdalla et al. 2022), as well as in other studies in environments with postfire erosion (Canfield et al. 2005, Goodrich et al. 2012, Villarreal et al. 2022).

One of the difficulties to represent the physics of runoff depth and sediment yield is to obtain the lateral inflow rate to a plane since it is not possible to measure directly. Usually, it is supposed that this lateral rate is a constant or satisfies a predefined function of the difference between the rainfall rate and the infiltration rate, generating uncertainties (Kim et al. 2014, Galina et al. 2018, An et al. 2019, Harche et al. 2021). There are few studies in the literature that consider the confidence intervals of rainfall-runoff modelling results (Al-Qurashi et al. 2008, Kennedy et al. 2013, Kim et al. 2014), however, an important justification would be the error performance criterion of the events (Atiquzzaman & Kandasamy 2016, Ossa-Moreno et al. 2019, Kautz et al. 2019).

In the Amazon, the search for climate change projection studies becomes increasingly urgent as the occurrence of large seasonal and inter-annual variations becomes increasingly intense and frequent (Sorribas et al. 2016, Costa et al. 2021). For a more specific analysis, we considered a catchment in the Amazon influenced by soil change activities, family farming and agribusiness; a catchment most vulnerable to climate change (Costa et al. 2021, da Silva Cruz et al. 2022). It is also clear that the Amazon has a high strategic value, as Brazil is highly dependent on its water resources for various economic development activities (Costa et al. 2020).

Thus, the goal of this work was to apply the method of inverse problems, which the novelty of the paper, to estimate parameters and the lateral inflow rate to simulate runoff depth in a small

catchment of the Amazon, where intense rainfall events occur, and to simulate flow and sediment yields, affecting rural populations. This study may also prove to be useful to demonstrate basins where measured data are limited.

NOMENCLATURE

A0, A1, A2, B1, B2 parameters of the model of the inverse problems (IP)
h runoff depth per unit area, mm
$h_u(L,t)$ depth at the lower boundary of the contributing plane at time t
I identity matrix
IP Inverse problem
k random variable with Gaussian distribution from Metropolis-Hastings algorithm
K2 Kineros2 – A Kinematic Runoff and Erosion Model
L length, m
MCMC Markov chain Monte Carlo
n Manning's coefficient
P* candidate parameter
q(x,t), q(t) lateral inflow rate, $mm.h^{-1}$
Q discharge per unit width, $mm.h^{-1}$
S slope
t Time
u subscript to the upstream surface
u* random number with Uniform distribution
W width, m
w search step

GREEK SYMBOLS

π(Data) probability distribution of the data
π(Data|P) likelihood function
π(P) prior probability distribution
π(P|Data) posterior probability distribution
φ Metropolis test
α and m soil parameters defined according to the slope roughness
ρ1 and ρ2 constants fitted to the data seen using Markov chain Monte Carlo (MCMC)

MATERIALS AND METHODS

Study Area

The study area is the Prata catchment, located in the municipality of Capitão Poço (Fig. 1) in northeastern Pará, Amazon, Brazil. The basin has a total area of 82 km2 flowing into the Guamá River. The climate corresponds to the Köppen classification "Am" (equatorial climate), characterized as rainy and with a short dry season between September and November. This catchment has been the subject of previous hydrological and hydro sedimentological studies (Blanco et al. 2013, Silva et al.

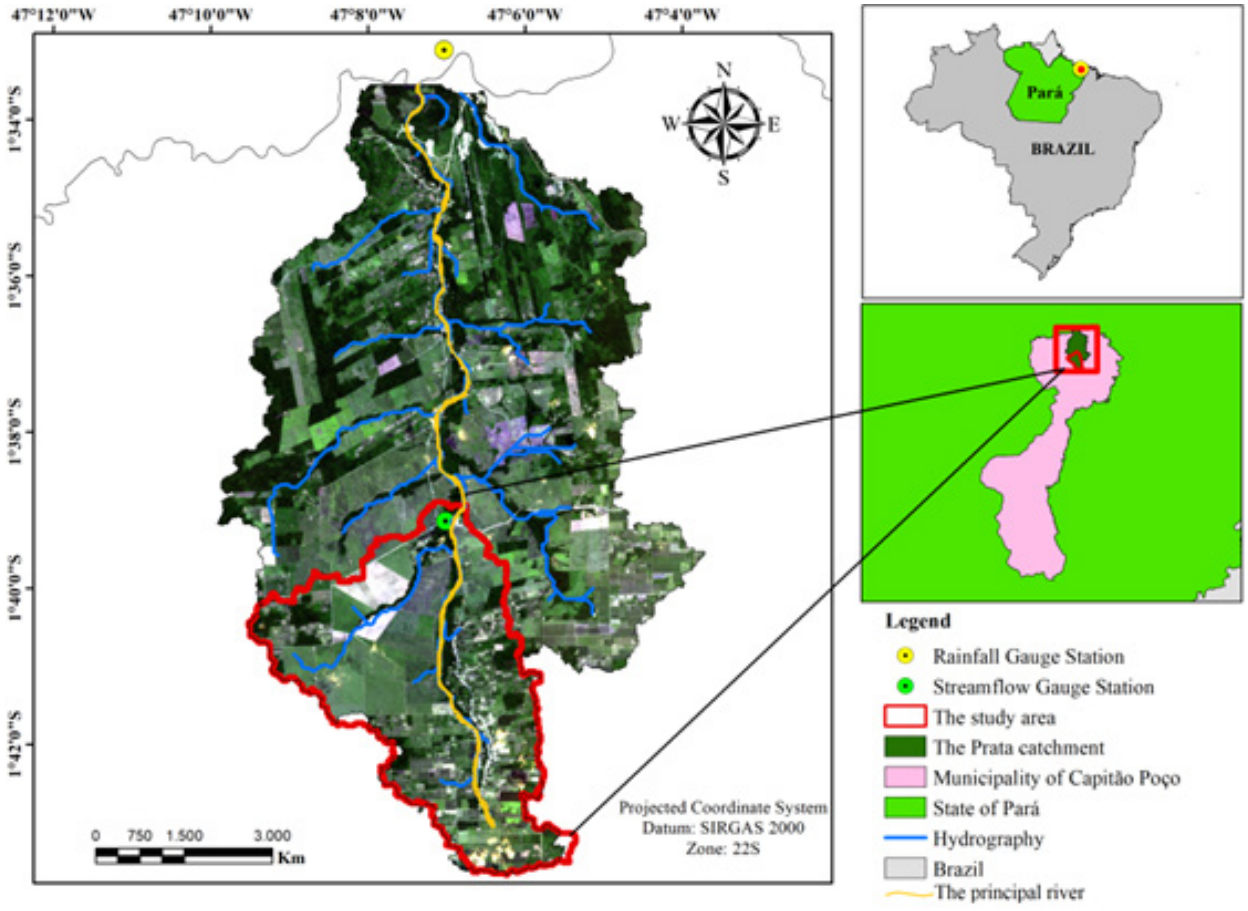

Figure 1. Location of the small catchment of the Amazon.

2020). The region has an average annual temperature of 26.9 °C, with minimums and maximums of approximately 21.4 °C and 32.7 °C, respectively, while the average relative humidity is approximately 83%. The annual rainfall is 2,370 mm, with the wettest months between January and June and the peak in March (Silva et al. 2020). Blanco et al. (2013) mention that the catchment has a long series of flow data; however, it does not have precipitation data. The streamflow data comes from the streamflow gauge station Marambaia, which is part of the HIDROWEB system (http://www.snirh.gov.br/hidroweb/) of the National Agency for Water and Basic Sanitation of Brazil (ANA). Thus, the main river of the small catchment of creek's Prata was considered in the KINEROS2 model (Fig. 1).

Direct Model - Kinematic Wave Model

Given the scarcity of data available on the National Agency for Water and Sanitation - ANA platform (http://hidroweb.ana.gov.br/) and the limitation of obtaining experimental/observed data in the watershed, the kinematic wave model was identified as the direct model (DM) is the model simulates the water sheet, flowing on the surface of the basin. Figure 2 summarizes the physical model of the kinematic wave, which is based on the continuity equation and is presented in Eqs. 1 and 2 (Lighthill & Whitham 1955, Chow 1959, Singh 1983, Chow et al. 1988, Woolhiser et al. 1990, Smith et al. 1995, Kim et al. 2014, Galina et al. 2018, Harche et al. 2021).

$$\frac{\partial h}{\partial t} + \frac{\partial Q}{\partial x} = q(x,t) \qquad (1.a)$$

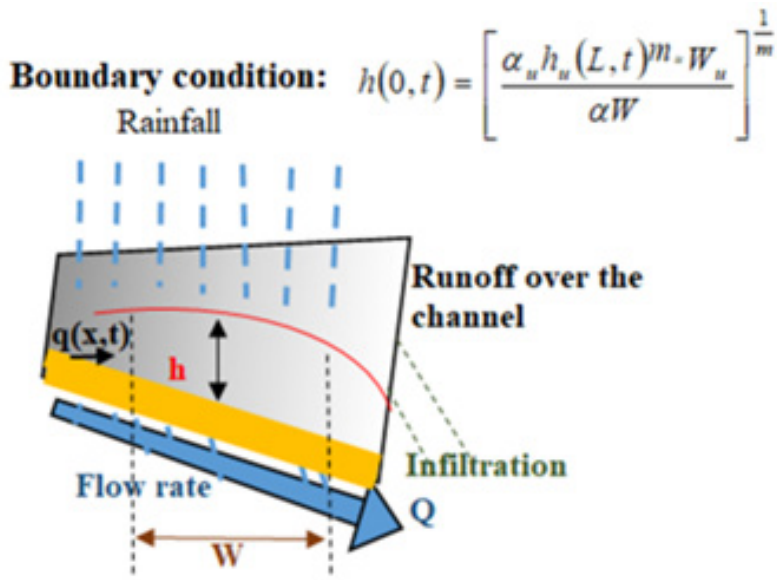

Figure 2. Representation of the kinematic wave model.

where Q is the discharge per unit width (mm/h), h is the runoff depth per unit area (mm) and q(x,t) is the lateral inflow rate (mm/h). The discharge Q can be represented by Eq. 1.b (Singh 1983, Walker & Humpherys 1983).

$$Q = \alpha h^m \tag{1.b}$$

$$\alpha = (\rho_1 S)^{1/2}/n \text{ and } m = \rho_2 \tag{1.c-d}$$

where α and m are soil parameters defined according to the slope roughness, ρ1 and ρ2 are constants fitted to the data seen using Markov chain Monte Carlo (MCMC), S is the slope, and n is Manning's coefficient.

The soil parameters of Eq. (1.c-d) are dimensionless. In this study, Eq. (1.c-d) was adapted from the K2 model, which considers values in this option: $\alpha = 1.49S^{1/2}/n$ and m = 5/3 (Woolhiser et al. 1990). However, ρ_1 and ρ_2 were inserted to represent the simulated observations via IP closest to the pseudo-observations obtained via K2. Combining Eqs. (1.a-d), results in Eq. 2.

$$\frac{\partial h}{\partial t} + \alpha m h^{m-1}\frac{\partial h}{\partial x} = q(x,t) \tag{2}$$

Equations 1 and 2 have the following boundary conditions (Eqs. 3 and 4) and initial condition (Eq. 5) (Singh 1983, Woolhiser et al. 1990, Smith et al. 1995, Galina et al. 2018). If the upstream boundary is a flow divide, the boundary condition (Eq. 3).

$$h(0,t) = 0 \tag{3}$$

$$h(0,t) = \left[\frac{\alpha_u h_u(L,t)^{m_u} W_u}{\alpha W}\right]^{\frac{1}{m}} \tag{4}$$

$$h(x,0) = 0 \rightarrow 0 \le x \le L\ ; \tag{5}$$

where $h_u(L,t)$ is the depth at the lower boundary of the contributing plane at time t, u is the subscript to the upstream surface, L is the length (m), and W is the width (m). Equation 4 is applied if

another surface is contributing flow at the upper boundary. It is important to emphasize the difficulty of determining the lateral inflow rate q(x,t) in the runoff process.

Direct Model Solution – The method of lines (MOL)

The direct model, applied to Eqs. (1-5), was solved using the method of lines (MOL – Fig. 3), where the partial differential equation is discretized and transformed into a system of coupled ordinary differential equations (Oymak & Selcuk 1996, Sadiku & Garcia 2000, Ismail et al. 2007, Shakeri & Dehghan 2008, Schiesser & Griffiths 2014, Roknujjaman & Asaduzzaman 2018). Figure 3 illustrates the applied discretization.

Applying centric differences and considering lagging differences in the lateral inflow rate term, the partial differential equation described in Eqs. (1-5) is presented by the following system of coupled ordinary differential equations.

$$\frac{\partial h_i}{\partial t} = q(x_i,t) - \alpha m h_i^{m-1} \frac{h_i - h_{i-1}}{\Delta x};\ 1 < i < N \qquad (6.a)$$

With the following boundary conditions,

$$i = 1\ (h = h0);\ h_i = \left[\frac{\alpha_u h_u(L,t)^{m_u} W_u}{\alpha W}\right]^{\frac{1}{m}} \qquad (6.b)$$

And initial,

$$hi = 0;\ 1 < i < N \qquad (6.c)$$

The modelling of the lateral inflow q(x,t) was elaborated through this model because direct measurements were not possible. Attempts to obtain this information were constant (Sing 1983) or as a predefined function of differences between the rainfall rate and the infiltration rate (Kim et al. 2014, An et al. 2019). Due to this difficulty, the lateral flow q(x,t) was modelled with inverse problems as a Fourier transform (Eq. 7) so that it depended only on the independent variable, i.e., time.

$$q(t) = A0+A1\sin(wt) + B1\cos(wt)+A2\sin(wt)+ B2\sin(2wt) \qquad (7)$$

KINEROS2 (K2)

KINEROS2 is a physical model that uses the equations of the kinematic wave model to be over rectangular planes and open channels through the platform's K2 program (https://www.tucson.ars.ag.gov/KINEROS/). The software uses three types of files: input (considers the parameters that describe the geometric, hydraulic, and infiltration characteristics of the basin); precipitation (considers rainfall data from the watershed), and output (shows the responses of rainfall rate, surface runoff, and

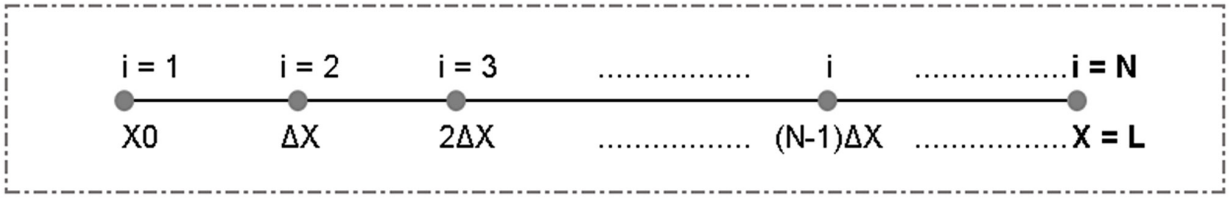

Figure 3. Representation of the method of lines (MOL).

sedimentation). The precipitation data are coolheaded on the work by Lima et al. (2014) and the rainfall station in the city of Ourém-PA (code: 00147016 - National Agency for Water and Sanitation - ANA). The physical parameters of the soil are calibrated in the K2 Software by successive approximations until the best value for each parameter is accepted so that the outputs of the hydrological rainfall-runoff simulation corroborate real scenario. It is noteworthy that the precipitation file of the KINEROS2 simulations includes a set of data generated (accumulated discretization every 6 minutes up to 2 hours) by the HUFF method (Huff 1967, Lu & Qin 2020). Figure 4 shows the representative sequence of K2.

The KINEROS2 model uses the equations of the kinematic wave model, establishing the solution of the water layer, which flows on the surface of the basin. However, depending on the geometric complexity, watersheds can be represented by a combination of planes, convergent section, divergent section and channel. A plan can be used to represent a study area or a part of it (Singh, 1983). This study will be limited to the case of a part of it (Fig. 1)

Following the procedure, an output file was obtained for the study area with observations of rainfall rate and simulated surface runoff and sediment yield. However, the lateral inflow rate cannot be explicitly validated. Hence, the data obtained in K2 can be used to solve the inverse problem method to estimate the lateral inflow rate and assess the influence of the optimized parameters for the runoff depth responses.

Method of Inverse Problems

Hydrological models have parameters that cannot be measured directly; therefore, inferences are made for their estimation. Thus, the Bayesian technique with Markov chain Monte Carlo (MCMC) was applied to estimate the parameters of the K2 model/direct model. When solving the physical model (Eqs. 1-5), the result is time series of runoff depth. This state variable (runoff depth) is the observable variable from which measurements can be obtained. The estimations were performed using MCMC in the simulation; where in this study Fourier transform (Eq. 7) was considered to represent q(t), the lateral inflow rate. In this form; this term is modelled more generally for any basin, because the direct model is obtained through the mass balance of the watershed. In this sense, applying the model to another basin, it is necessary to estimate parameters with the data or output that you want to represent through simulations. Therefore, to fill gaps in rainfall data and the lateral inflow rate in the watershed of interest, this observable variable (runoff depth) was applied to find the model parameters (Fig. 5).

Figure 5 presents the representation of IP in hydrological modeling. The IP combines information from the observed data and the mathematical model simultaneously. In the initial analysis, as part of the K2/DM model, the following model inputs were considered: physical parameters and precipitation data; resulting in simulated observations via DM-IP and pseudo-observations via K2. Similarly, following the analysis of simulated versus observed data, the application of the IP (using a Bayesian structure and a Fourier transform, respectively) was considered to estimate the model parameters and the lateral input rate (unknown variable). From this, the 95% CI was performed and, in sequence, the performance evaluation; obtaining the output of interest for the study, i.e., runoff depth.

FILE I: File_input.f

```
BEGIN GLOBAL

 CLEN = 423,  UNITS = METRIC
 DIAMS = .005, .05, .25 ! mm
 DENSITY = 2.65, 2.60, 2.60 ! g/cc
 TEMP = 33 ! deg C
 Nele = 2
END GLOBAL
!-------------------------------------------------------
BEGIN PLANE
 ID = 1,  LEN = 400,  WID = 200,  SL = .005,
 CV = .12,  THICK = 500,  SAT = .2,  PR = 2
 RELIEF = 2,  SPACING = .3
 KS      G      DIST   POR      ROCK
 2.6     12.7   0.45   .38     0      ! upper layer
0.43     26.3   0.39   .32     0      ! lower layer
 FRACT = 0.2, 0.6, 0.2  SPLASH = 50, COH = 0.5
 Plot = H
END PLANE
!-------------------------------------------------------
BEGIN CHANNEL
 ID = 2,  LAT = 1,  LEN = 400,  PR = 2
 DEPTH = 1.0
 WIDTH = 200, SLOPE = .005, MANNING = .15,
 COH = .01,  FRA = 0.0, 0.4, 0.6
 PAV = 0.6
 Plot = H
END CHANNEL
```

FILE II: Precipitation.f

```
BEGIN     RG001
          N =        21
          TIME       DEPTH
!         (min)      (mm)
          0.0        0.00
          6.0        18.10
          12.0       37.40
          18.0       48.70
          24.0       58.90
          30.0       68.00
          36.0       74.80
          42.0       80.40
          48.0       85.00
          54.0       89.50
          60.0       92.90
          66.0       95.20
          72.0       97.40
          78.0       99.70
          84.0       102.00
          90.0       104.20
          96.0       106.50
          102.0      108.80
          108.0      109.90
          114.0      111.00
          120.0      113.30
END
```

FILE III: File_output.f

Time (min)	Rainfall (mm/h)	Outflow (mm/h)	Outflow cu (m/s)	Total Sediment (kg/s)
0	185.80	0.00	0.00	0.00
10	126.80	0.19	0.04	0.21
20	95.40	2.12	0.47	3.86
30	63.20	7.69	1.71	40.60
40	47.80	15.69	3.49	138.48
50	38.40	23.43	5.21	276.52
60	22.60	29.98	6.66	422.62
70	22.80	35.24	7.83	555.23
80	22.40	39.09	8.69	656.50
90	23.00	41.42	9.20	714.14
100	13.40	42.06	9.35	720.28
110	18.20	40.98	9.11	675.82
120	0.00	38.59	8.58	596.96
130	0.00	35.37	7.86	500.84
140	0.00	31.68	7.04	399.26
150	0.00	27.98	6.22	327.74
160	0.00	24.54	5.45	436.13
170	0.00	21.46	4.77	359.35
180	0.00	18.75	4.17	293.28
190	0.00	16.40	3.65	239.57
200	0.00	14.38	3.20	196.72
210	0.00	12.64	2.81	162.63
220	0.00	11.14	2.47	135.43
230	0.00	9.84	2.19	113.60
240	0.00	8.72	1.94	95.95
250	0.00	7.75	1.72	81.60
260	0.00	6.91	1.54	69.83
270	0.00	6.18	1.37	60.11
280	0.00	5.53	1.23	52.04
290	0.00	4.97	1.10	45.28
300	0.00	4.47	0.99	39.61

Figure 4. Representation of input and output K2 (Woolhiser et al. 1990).

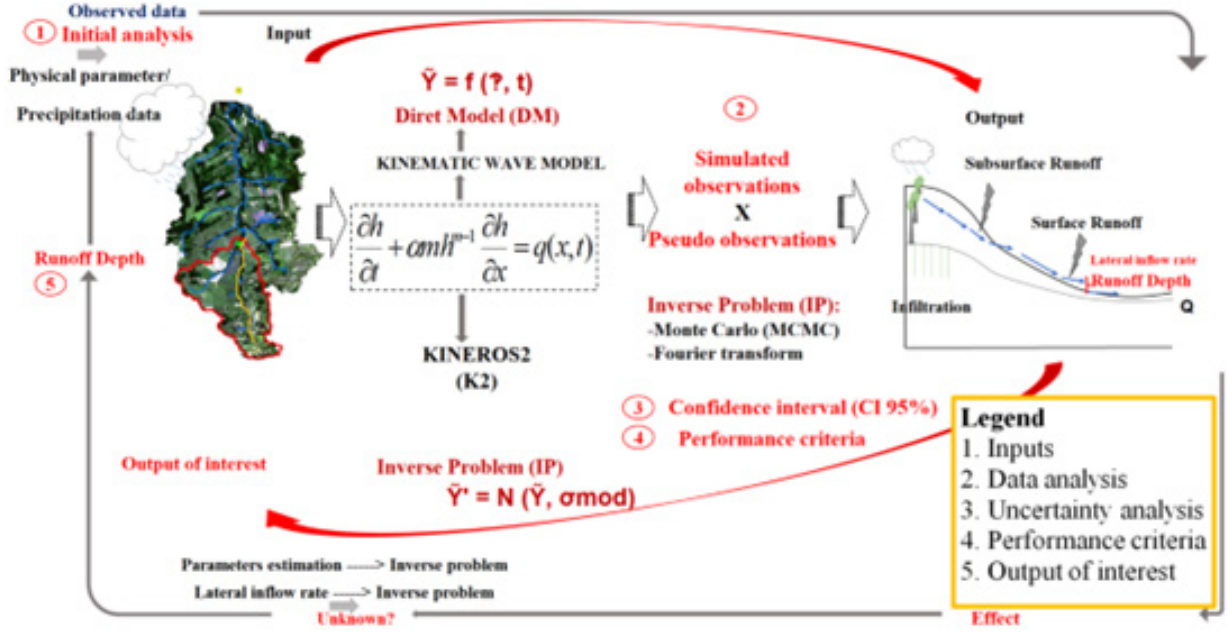

Figure 5. Representative drawing of hydrological modelling based on the inverse problem method.

Bayes' Theorem – Markov Chain Monte Carlo (MCMC)

In many problems, it not possible to have reliable observations or make direct measurements. These hydrological gaps can be filled using information about possible measurements with mathematical formulation (direct problem) and a priori knowledge of model parameters. This mathematical problem can be addressed using by Bayes' theorem, the posterior distribution π (P|Data) being considered,

as the probability of prior distribution π (P) by likelihood of π (Data|P), and under the marginal probability distribution π (Data) - (Beck & Arnold 1977, Kaipio & Somersalo 2006, Oliveira et al. 2020, Moura et al. 2021, 2022, Amador et al. 2022).

The estimation of the parameters of the physical model from observed data is a prerequisite for the modelling of the flow process (Canfield et al. 2005, Al-Qurashi et al. 2008, Kennedy et al. 2013, Kim et al. 2014). The Bayesian estimation method quantifies the discrepancy by a multiplicative factor while obtaining the probability distributions of a single set of physical parameters. In this work, the inverse problem was applied to surface runoff, and 4 different events were evaluated using hydrological modelling. The parameters of the model of the inverse problems (IP) are PT = [W W_u α αu Ω A0 A1 A2 B1 B2], where (W: width of the downstream plane - m; W_u: width of the contributing plane - m; α and α_u: parameter referring to watershed properties, including slope: S, Manning roughness coefficient: n; coefficients: ρ1 and ρ2; Ω; and the parameters of the Fourier transform used, A0, A1, A2, B1, B2 – Eq. 7).

The Bayesian technique used to estimate the parameters was the MCMC method, which can be implemented using different algorithms of acceptance/rejection, for example, Gibbs and Metropolis–Hastings. In this study, the Metropolis–Hastings accept/reject algorithm was implemented, and candidate parameters were generated, considering random walk as the transition kernel. The algorithm is as follows (Hastings 1970, Beck & Arnold 1977; Oliveira et al. 2020, Nunes et al. 2021, Viegas et al. 2022, Nunes et al. 2022):

The Markov chain iteration counter is initialized (i = 0), and a value is arbitrarily pick for the first estimate of the parameter P^0.

A candidate value P* is generated through a transition kernel, Eq. 8, where k is a variable N (0,1) and w is the search step.

$$P^* = (I + wk)\, Pi\text{-}1 \tag{8}$$

I is the identity matrix.

1) The probability of acceptance (φ) of the candidate parameter is calculated using the Metropolis test (Eq. 9).

$$\phi = \min\left[1, \frac{\pi(P^* / Observed)}{\pi(P^{(i-1)} / Observed)}\right] \tag{9}$$

2) Generate a random number u* from a uniform distribution, u* ~ U (0,1).
3) If U ≤ α, then the new value is accepted and $P^i = P^*$. Otherwise, reject and make $P^i = P^{i-1}$.
4) Increment the counter from i to i+1 and return to step 2.

Performance criteria

Since observations were not available, pseudo-observations were obtained with the aid of K2 software, which is necessary to supply information on precipitation data and parameters referring to the basin. In order to assess the agreement between the experimental/observed and predicted data; for performance evaluation, based on works by Moraes Cordeiro & Blanco (2021) and Costa et al. (2021) in the Amazon region, five statistical criteria were used, Pearson's coefficient (r) (Duan et al. 2015) presented in Eq. 10; the coefficient of determination (R2) (Cheng et al. 2014) presented in Eq. 11; the Nash-Sutcliffe coefficient (NSE) (Nash & Sutcliffe 1970) presented in Eq. 12; in this case, the closer

to unity, the better the fit between observable and predicted data. The root mean square error (RMSE) (Gebremicael et al. 2019) presented in Eq. 13; and the percentage bias (PBIAS) presented in Eq. 14. The RMSE penalizes errors of greater magnitude (Moraes Cordeiro & Blanco 2021).

$$r = \frac{\Sigma_{i=1}^{n}(h_i^{OBS} - h^{\bar{O}BS})(h_i^{SIM} - h^{\bar{S}IM})}{\sqrt{\Sigma_{i=1}^{n}(h_i^{OBS} - h^{\bar{O}BS})^2}\sqrt{\Sigma_{i=1}^{n}(h_i^{SIM} - h^{\bar{S}IM})^2}} \quad (10)$$

$$R^2 = \frac{\{\Sigma_{i=1}^{n}(h_i^{OBS} - h^{\bar{O}BS})(h_i^{SIM} - h^{\bar{S}IM})\}^2}{\Sigma_{i=1}^{n}(h_i^{OBS} - h^{\bar{O}BS})^2 \Sigma_{i=1}^{n}(h_i^{SIM} - h^{\bar{S}im})^2} \quad (11)$$

$$NSE = 1 \frac{\Sigma_{i=1}^{n}(h_i^{OBS} - h_i^{SIM})^2}{\Sigma_{i=1}^{n}(h_i^{OBS} - h^{\bar{O}BS})^2} \quad (12)$$

$$RMSE = \sqrt{\frac{1}{n}\Sigma_{i=1}^{n}(h_i^{OBS} - h_i^{SIM})^2} \quad (13)$$

$$PBIAS = \frac{\Sigma_{i=1}^{n}(h_i^{OBS} - h_i^{SIM}) * 100}{\Sigma_{i=1}^{n}(h_i^{OBS})} \quad (14)$$

where n = number of observations at each time step; h_i^{OBS} = observed data; $h^{\bar{O}BS}$ = average of observed data; h_i^{SIM} = simulated data and $h^{\bar{S}IM}$ = average of simulated data.

The logical structure of the method used in the study is shown in Fig. 6.

The IP combines information from the observed data and the mathematical model simultaneously. The KINEROS2/Direct Model (DM) model uses the kinematic wave equations and the mass balance equation to represent the processes of runoff and sedimentation (Singh 1983, Woolhiser et al. 1990, Smith et al. 1995). The approach of this study, estimating the runoff depth and the lateral inflow rate, used the kinematic wave model equation along with the IP, as direct measurements were not possible (Fig. 6).

RESULTS AND DISCUSSION

The results are presented in the following order: i) generation of pseudo-observations of the outflow by K2; ii) results from the generation of indirect measurements by the MCMC and Fourier; iii) results of the uncertainty analysis of the parameters and performance evaluation of the modelling; and iv) the optimized runoff depth results.

Outflow K2

Table I presents the results of the physical parameters calibrated in K2 for maximum/daily events [A (04/14/2011); B (04/09/2012a); C (04/09/2012b); and D (22/03/2013)] of accumulated rainfall, equal to 113.3, 56.7, 54.6 and 63.8 mm, respectively.

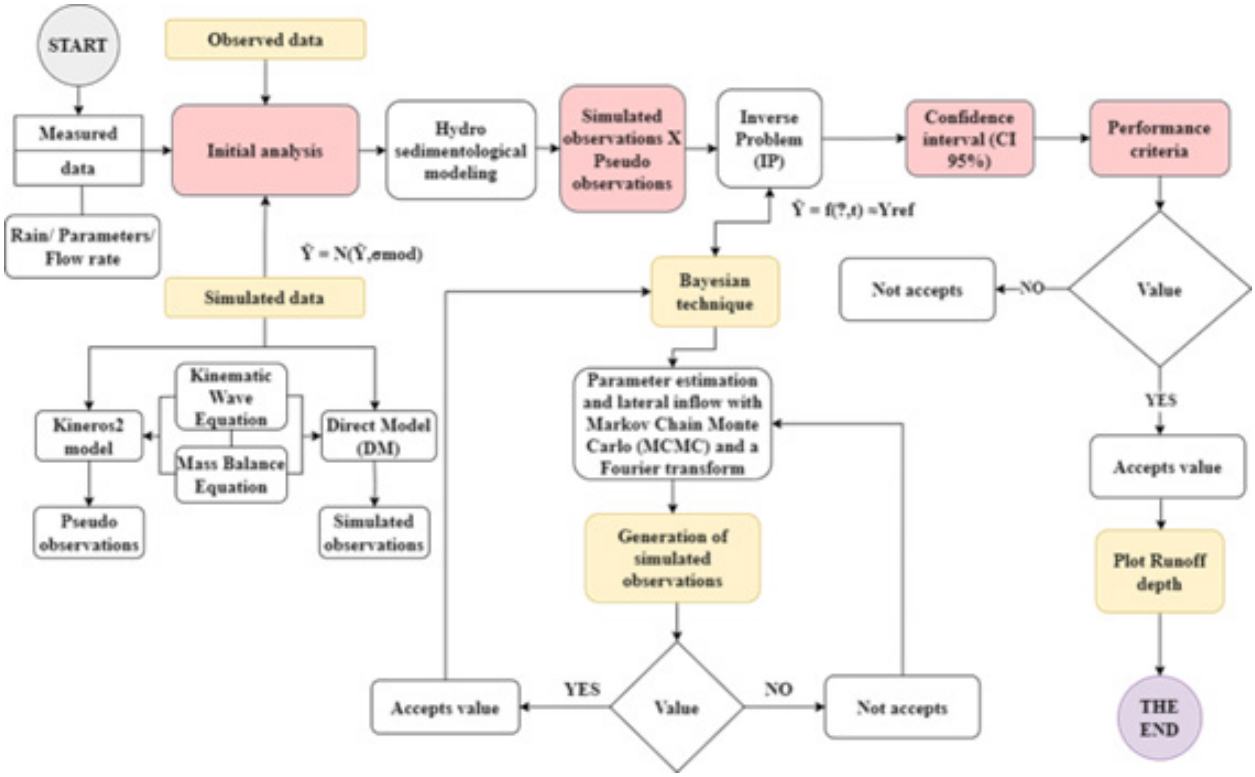

Figure 6. Schematic flowchart of the steps of the inverse problem method.

The values of parameters n, Ks, Cv, and G are consistent with the study by Memariam et al. (2012) for tropical basins, where the values used were between n (0.00-1.04), Ks (0.01-0.60), Cv (0.00-0.12) and G (0.00-2.68). In this sense, there are also case studies that used similar slope and width parameters (S [0.0004-0.023] and W [16.8-61.0]) for watersheds with physical characteristics, tropical climatic conditions and intensive land use, prone to severe flooding and with limited data available (Nguyen et al. 2015, Mirzaei et al. 2016).

For the physical parameters studied, seven had considerable influences on the outputs: S (0.01-1.0), Si (0.0-1.0), n (0.01-0.8), Ks (0-50), Cv (0.01-50), G (0.0-500.0) and λ (0.01-1.43). Thus, the results agree with those available in the literature for basins with predominantly flat relief, sandy loam and sandy soil texture (characteristics that influence Ks), intensive agriculture (Kim et al. 2014), and slopes between 1% and 20% (Al-Qurashi et al. 2008, An et al. 2019). Slope is a parameter that influences the flow response speed. However, what caught our attention was the influence of some parameters on the outputs of K2 (Fig. 7), for example, S (0.05-1.0), n (0.01-0.1), Ks (0-50), and G (0.0-500.0). Figure 7 also shows the runoff depth peaks as a function of time for the four rainfall events of this study. Figure 7 is represented using the values from Table I.

Even with similar calibrated physical parameters, the peaks of the hydrographs changed due to different inputs of accumulated precipitation. Therefore, the causes of changes in outputs may also be due to the speed of responses (automatic interpolation) by K2 (Woolhiser et al. 1990, Goodrich et al. 2012, Abdalla et al. 2022). The values presented in Fig. 7 considered the outflow at the catchment outlet (Fig. 1). However, in terms of outflow variability, the events showed an almost homogeneous behaviour (B, C, and D) between the runoff depth results represented in K2, but event A presented

Table I. Identification of K2 parameters.

Parameter	Symbol	Units	Values used in the study	Values suggested	Estimation method/ Reference
Length	L	m	3000	-	Field measurements
Width	W	m	20	-	Field measurements
Slope	S	-	0,025	0-1	Kim et al. 2014
Density	Ss	-	0.80-1.50	0-2.80	An et al. 2019
Thickness	Thick	mm	300	0-500	An et al. 2019
Soil porosity	ϕ	-	0.38	0-45.77	Al-Qurashi et al. 2008, An et al. 2019
Saturation initial	Si	-	0,2	0-1	Kim et al. 2014, An et al. 2019
Manning	n	-	0,3	0.01-0.8	Memariam et al. 2012, An et al. 2019
Saturated hydraulic conductivity	Ks	$mm.hr^{-1}$	0.60	0-50	Al-Qurashi et al. 2008, Memariam et al. 2012
Coefficient of variation of Ks	Cv	-	0.1	0.01-50	Memariam et al. 2012, Kim et al. 2014
Mean capillary drive	G	mm	12.70	0-500	Memariam et al. 2012, An et al. 2019
Pore size distribution index	λ	mm	0.45	0.03-1.43	Kim et al. 2014, An et al. 2019
Rainsplash coefficient	Cf	-	0	0-625, 2500, 5625	An et al. 2019
Soil cohesion coefficient	Co	-	0.5	0.001-0.1	An et al. 2019
Micro topographic Relief	re	mm	2	0-400	Kim et al. 2014
Micro topographic Spacing	rs	m	0.3	0.001-10	Al-Qurashi et al. 2008, Kim et al. 2014
Rock cover	r	%	0-1	0-1	An et al. 2019
Interception depth	In	mm	1.0	0.01-300	Kim et al. 2014
Plant cover	p	%	0-1	0-1	An et al. 2019

a considerable difference in the output. However, unlike the other events (B, C and D), event A can be an indicator of the climatic extremes that occur in the Amazon region. Thus, understanding the effects of climate variability on the hydrological cycle is fundamental for government development plans, mainly because extreme hydroclimatic events can have a strong influence not only in the environmental aspect, but also in the socioeconomic aspect. In the Amazon, the search for climate forecast studies becomes increasingly urgent, as the occurrence of large seasonal and interannual variations becomes increasingly intense and frequent (Costa et al. 2021).

Overall, the K2 responses showed a slight difference in the peak time of the hydrographs (from 100 to 140 minutes) due to different rainfall inputs automatically interpolated based on the space-time relationship, as shown by Woolhiser et al. (1990). These results, with variable responses and differences in calculated water peaks, are justified by Araújo et al. (2013), Kennedy et al. (2013), Kim et al. (2014), and An et al. (2019). The authors credit this to the nonlinearity of the model, interpolated

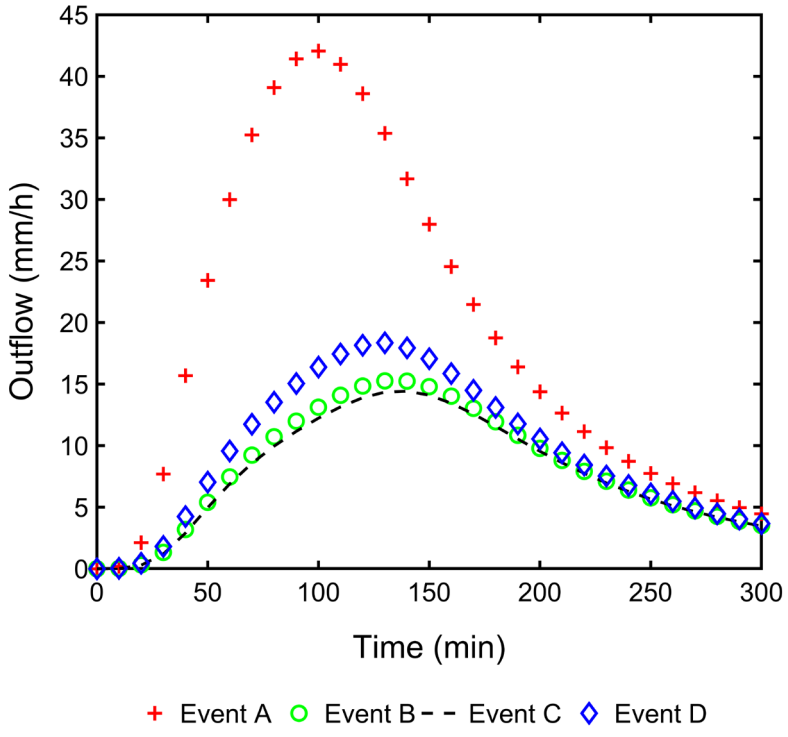

Figure 7. Outflow of events represented with the K2 model.

precipitation data, and unsatisfactory performance of showing the best parameter values in the calibration process.

Generation of indirect measures

Parameter estimation with MCMC

Table II presents the values of the parameters generated with the IP as a function of the maximum rainfall events/day (A, B, C, and D).

The parameters obtained via IP are the results of the estimation with MCMC given the values reported in Table 1, being put in two groups: physical parameters K2 [W; W_u; α and α_u (i.e., S and n)]; and physical parameters (Ω, A0, A1, A2, B1, B2) of the DM/IP, derived from the Fourier transform used (Eq. 7). Thus, these sets of parameters simulated the lateral inflow rate and represented the runoff depth (Fig. 8). Overall, the estimation of parameters using MCMC was able to quantify their reliability, as well as, the scenarios, and models, in addition to being used for sampling and characterizing the solution of an IP (Kaipio & Somersalo 2006).

According to Hastings (1970), Beck & Arnold (1977), Oliveira et al. (2020), Nunes et al. (2021), and Viegas et al. (2022), the purpose of parameter estimation with MCMC was to provide the model with a gradual convergence to an equilibrium distribution, i.e., the Markov chain becomes more stable, having standardized parameter values. In this context, the results of the best values of Table II were considered a local sensitivity analysis with up to 3000 states of the Markov chain around the standard values of Table 1. In this process of parameter standardization of IP, an approximate simulation time of twenty minutes was registered for each catchment event. Thus, as expected, the

Table II. Parameter estimates through the IP developed for each event evaluated.

Parameter		Optimal values with IP per event			
		Event A	Event B	Event C	Event D
Upstream width	W_u	13.49	17.935	14.142	16.104
Width	W	10.826	9.469	9.378	9.711
Upstream slope and roughness	α_u	112.672	147.632	158.668	149.114
Slope and roughness	α	7.394	6.179	6.278	6.671
Fourier transform coefficients	Ω	0.009	0.009	0.009	0.009
	A0	0.456	0.438	0.462	0.458
	A1	41.189	39.702	39.609	41.182
	B1	26.673	16.947	15.872	17.186
	A2	15.28	14.866	14.189	14.404
	B2	2.12E-04	2.33E-04	2.13E-04	2.32E-04

parameter estimates depended on the perturbations (chain states) made in the first values of the parameters (Al-Qurashi et al. 2008, Kennedy et al. 2013, Kim et al. 2014).

Runoff depth and lateral inflow rate estimates

Figure 8 shows the responses of the runoff depth developed with K2 and IP and the simulation of the lateral inflow rate obtained with IP as a function of the maximum/daily precipitation events (A, B, C, and D) evaluated around the study area. The runoff depth and lateral inflow rate responses are the results of the interactions of the inputs obtained in K2 (observable data) and of the standardized parameters with MCMC and Fourier in rainfall-runoff modelling when trying to represent the existing scenario closer to the catchment. After the process of estimating the parameters via IP, the occurrences of lateral rate variability in the outflow responses showed little variable behaviour close to the observed measurements at K2. In this sense, the IP simulations showed a slight difference in the representation of the runoff depth with respect to the K2 responses. The considerable difference is in event A, with the highest peak volume; is due to possible variations in the input data obtained with K2 (Woolhiser et al. 1990) and the nonlinearity of the direct model (Lighthill & Whitham 1955, Singh 1983, Woolhiser et al. 1990, Smith et al. 1995). However, other studies addressing rainfall-runoff modelling cite that the lateral inflow rate estimate may handle errors and changes in the flow sheet representation (Singh 1983, Kim et al. 2014, An et al. 2019).

According to Woolhiser & Goodrich (1988), water flowing from the planes enters the main channel in the form of a lateral inflow rate. Therefore, it is important to estimate the values of this influence on the outflow, which may result from changes in land use and cover. In this sense, our results with the IP estimated the lateral inflow rate, serving as a surrogate to reduce costs and time in experimental tests to quantify the flow process. As analysed in other studies (Nguyen et al. 2015, Mirzaei et al. 2016), K2 alone does not accurately estimate the water level of the river, a key variable to characterize flash floods. Thus, using K2 together with the IP method, it became possible to simulate the lateral entry

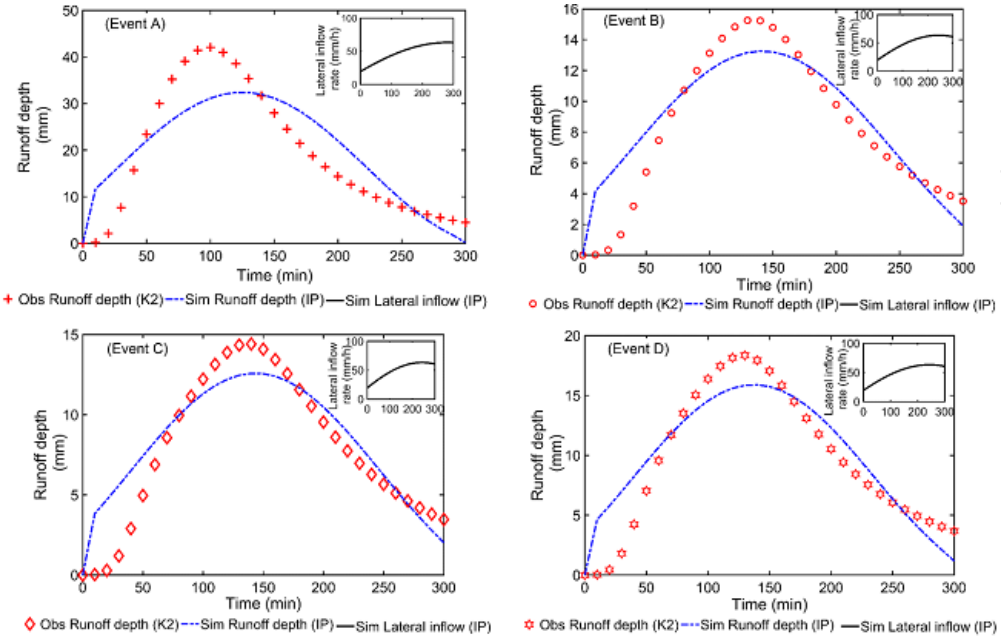

Figure 8. The runoff depth K2/IP responses (observed/simulated) and lateral inflow rate (simulated) as a function of time for the four maximum/daily rainfall events.

rate and show this influence on changes in the behaviour of the runoff depth, as mentioned by Singh (1983) and Kim et al. (2014). Thus, the quality of adjustment of the lateral rate of Fig. 8 can be verified in the practical sense of applying the inverse solution (Araújo et al. 2013).

However, in the analysis of the peak times of the K2/IP responses, event C presented a considerable delay in peak time (more than 130 minutes). According to Kennedy et al. (2013) and Kim et al. (2014), the differences and delays associated with K2 and IP responses may be due to standardized parameter values and known or input data (Harche et al. 2021). Peak time considerations and knowledge of runoff depth variability are appreciable in structural designs to control flooding, erosion, and soil nitrogen loss (Lange & Haensler 2012, An et al. 2019, Kautz et al. 2019, Korgaonkar et al. 2020).

Uncertainty analysis and performance evaluation

Table III presents the values of the K2/IP physical parameters for each maximum/daily event with a 95% confidence interval (CI).

The parameters, considering a 95% confidence interval, are average (best) values and threshold values that simulated the outflow via IP closest to the outputs of K2 (i.e., pseudo-observations). Thus, these values represent a considerable degree of reliability in hydrological modelling (Fig. 8). In this context, the results of the uncertainty analysis of the events evaluated were compared to verify their consistency (NSE ≥ 0.75) (Goodrich et al. 2012, Harche et al. 2021) and their strengths in real hydrological situations (Walker & Humpherys 1983, Sanso & Guenni 2000). Good practices in hydrological modelling require that the modeller provides a reliable assessment of the parameters and the model, evaluating the possible uncertainties associated with the simulation process (Sanso & Guenni 2000, Al-Qurashi et al. 2008, Kim et al. 2014, An et al. 2019).

Analysing Table IV, the NSEs demonstrate satisfactory performance for the rainfall-runoff events modelled through IP and PBIAS demonstrate very good performance (An et al. 2019, Harche et al. 2021, Costa et al. 2021). The results of the IP were consistent with those of the studies. Considering the peak and duration of the hydrographs, such as wave delays, it is assumed that the series IP present

Table III. Physical parameters K2/IP variable as a function of the Fourier transform used and evaluated with a confidence interval of 95%.

Events		Parameters K2/IP									
		W	W_u	α	$α_u$	Ω	A0	A1	B1	A2	B2
Range		0-50	0-50	0-200	0-200	0-0.01	0-0.5	0-50	0-50	0-50	0-0.01
A	Average	13.49	10.83	112.67	7.39	0.009	0.46	41.19	26.67	15.28	2.12E-04
	CI 95%	13.4-13.5	10.8-10.9	112.6-112.7	7.3-7.4	0.008-0.009	0.45-0.46	41.18-41.19	26.6-26.7	15.2-15.3	2.12E-04-2.13E-04
B	Average	17.93	9.47	147.63	6.18	0.009	0.44	39.7	16.95	14.87	2.33E-04
	CI 95%	17.7-18.1	9.32-9.60	145.5-148.9	6.10-6.25	0.008-0.009	0.43-0.44	38.11-40.62	15.8-18.3	14.6-15.1	2.31E-04-2.36E-04
C	Average	17.14	9.38	158.67	6.28	0.009	0.46	39.61	15.87	14.19	2.13E-04
	CI 95%	16.9-17.4	9.28-9.51	153.5-164.1	6.21-6.34	0.008-0.009	0.45-0.47	38.35-41.18	14.8-17.0	13.9-14.6	2.11E-04-2.15E-04
D	Average	16.1	9.71	149.11	6.67	0.009	0.46	41.18	17.19	14.4	2.32E-04
	CI 95%	16.0-16.2	9.60-9.84	143.7-156.7	6.61-6.72	0.009	0.45-0.46	39.28-43.02	16.0-18.5	14.3-14.5	2.30E-04-2.34E-04

Table IV. Performance results at events.

Events	r	R^2	NSE	RMSE	PBIAS
A	0.88	0.77	0.76	6.72	-3.35
B	0.93	0.86	0.83	1.95	-5.32
C	0.93	0.87	0.84	1.80	-5.38
D	0.93	0.86	0.85	2.25	-3.88

values smaller than the pseudo observed ones in relation to K2. Even, the performance criteria r, R2 and RMSE, based on the ideal metric values, are consistent with the values of the work by Moraes Cordeiro & Blanco (2021) ($r \leq 1.00$, $R^2 \leq 1.00$, RMSE ≥ 0.00). Thus, the applied IP method can be used to predict the runoff depth responses and lateral inflow rates for small watersheds. Obtaining direct measurements is especially limited (Sanso & Guenni 2000, Al-Qurashi et al. 2008, Kennedy et al. 2013, Kim et al. 2014).

Optimization of the outflow uncertainty

After the uncertainty analysis process (CI = 95%) from Table III and performance evaluation with Nash-Sutcliffe from Table IV, the results of statistical correlation (R^2) showed a difference in the

trends of the runoff depth compared to the solution observable in K2. The considerable difference was for event A, with the lowest statistical correlation result (R^2 = 0.77), although considered a good result. The results of R2 of events B, C, and D showed a better fit in the rainfall-runoff modelling of the watershed, with results of 0.86, 0.87, and 0.86, respectively. This validates the methodological framework based on development of rainfall prediction solutions and unavailable data estimates, applying MCMC and Fourier transform as inverse methods (Sanso & Guenni 2000).

Although the K2 is a consolidated physical model in the literature and the simulations are for scenarios of observed hydrological data gaps (runoff depth and lateral inflow rate), the IP presented satisfactory efficiencies when comparing the performance criteria r, R^2, NSE and RMSE and the K2 simulations of the maximum accumulated rainfall events in the region.

CONCLUSIONS

The analysis of data from maximum/daily rainfall events, modelled with IP, shows good precision and reliability, as Nash-Sutcliffe coefficients and determination coefficients considered very good for events A, r = 0.88, R^2 = 0.77, NSE = 0.76 e RMSE = 6.72; B, r = 0.93, R^2 = 0.86, NSE = 0.83 e RMSE = 1.95; C, r = 0.93, R^2 = 0.87, NSE = 0.84 e RMSE = 1.80 e D, r = 0.93, R^2 = 0.86, NSE = 0.85 e RMSE = 2.25. The rainfall-runoff simulations largely depended on the determination of a suitable parameter values.

It is important to highlight that the results of the estimates of the runoff depth and the lateral inflow rate of the maximum/daily rainfall events A, B, C, and D showed reliability in the responses of the pseudo observations using KINEROS2 and simulated observations using IP, with a degree of reliability equal to 95%. The lateral inflow rate and the parameters that interacted were estimated using the behaviour of the rainfall-runoff modelling.

The lateral inflow rate, more generally modelled as a Fourier transform, can represent any watershed when obtained through the mass balance equation and parameter estimates with the data to be represented through simulations. Thus, the quantification of the reliability of the responses of the modelled physical processes is fundamental in the socioenvironmental management of rural and urban regions.

Rainfall-runoff modelling with applications of inverse problems is workable for real scenarios of physical processes and as part of a system of hydrometeorological data estimates to contribute to management and socioenvironmental control (flood and soil degradation); they interact satisfactorily in the adjustment process. Inverse problems (from the most rigorous at a statistical level to the least formal) can be workable to analyse changes in hydrological processes.

However, the method may present uncertainties in precise measurements, uncertainties that can be justified by the identification of the best numerical values of the parameters in the standardization process. In this context, the study of inverse problems in hydrology promotes the adaptation of indirect rainfall measures, lateral runoff rate estimates, and unavailable data estimates as a sustainable practice of cost and time reduction. In this case, the inverse problems can be considered as a tool to help reduce costs and time in the hydrological modelling with the scarcity of data and limitation of direct measurements.

As a suggestion for future studies, the application of inverse problems to other physical processes in hydrology, analysis of modelling behaviour and evaluation of parameters influencing the responses

of the models, uncertainty analysis, analysis of the information matrix, and the autocorrelation between the model parameters, as well as the input data in the probability distributions used as priors, are proposed as a solution to problems of identification of direct and indirect causes in hydrological processes to understand how they influence the results posteriorly.

Acknowledgements

The authors would like to thank the Coordination for the Improvement of Higher Education Personnel - Brazil (CAPES) - Finance Code 001. The second author would like to thank Conselho Nacional de Desenvolvimento Científico e Tecnológico (CNPq) for funding research productivity grant (Process 308147/2021-9). We would like to thank the office for research (PROPESP) and Foundation for Research Development (FADESP) of the Federal University of Pará through grant no. PAPQ 2022. The findings and conclusions in this article are those of the authors and do not necessarily represent the views of the Improvement of of Higher Education Personnel - Brazil (CAPES), or the CNPq for funding research productivity grant. The authors declare no competing interests.

REFERENCES

ABDALLA MAI, EL-WAHAB MA, TAWFIK M & KHATER I. 2022. Hydrological Models Simulation in Agricultural Watershed of Wadi Kharouba in North-Western Coast Region – Egypt. Fresen Environ Bull 31(01A/2022): 1063-1078.

AMADOR ICB, NUNES KGP, DE FRANCO MAE, VIEGAS BM, MACÊDO EN, FÉRIS LA & ESTUMANO DC. 2022. Application of Approximate Bayesian Computational technique to characterize the breakthrough of paracetamol adsorption in fixed bed column. Int Comm Heat Mass Transfer 132: 105917. https://doi.org/10.1016/j.icheatmasstransfer.2022.105917.

AL-QURASHI A, MCINTRYE N, WHEATER H & UNKRICH C. 2008. Application of the KINEROS2 Rainfall-Runoff Model to an Arid Catchment in Oman. J Hydrol 355: 91-105. https://doi.org/10.1016/j.jhydrol.2008.03.022.

AN M, HAN Y, XU L, XIURU W, AO C & PANG D. 2019. KINEROS2-based simulation of total nitrogen loss on slopes under rainfall events. CATENA 177: 13-21. https://doi.org/10.1016/j.catena.2019.01.039.

ARAÚJO ADS, VELHO HFC & GOMES VVF. 2013. Calibrating an hydrological model by an evolutionary strategy for multi-objective optimization. Inv Probl Sci Eng 21(3): 438-450. https://doi.org/10.1080/17415977.2012.712530.

ATIQUZZAMAN M & KANDASAMY J. 2016. Prediction of hydrological time-series using extreme learning machine. J Hydroinf 18: 345-353. https://doi.org/10.2166/hydro.2015.020.

BECK JV & ARNOLD KJ. 1977. Parameter estimation in Engineering and Science. New York: Wiley.

BLANCO CJC, SANTOS SSM, QUINTAS MC, VINAGRE MVA & MESQUITA ALA. 2013. Contribution to hydrological modelling of small Amazonian catchments: application of rainfall–runoff models to simulate flow duration curves, Hydrol Sci J 58(7): 1423-1433. https://doi.org/10.1080/02626667.2013.830727.

CANFIELD HE, GOODRICH DC & BURNS IS. 2005. Selection of Parameters Values to Model Post-Fire Runoff and Sediment Transport at the Watershed Scale in Southwestern Forests. Managing Watersheds for Human and Natural Impacts. https://doi.org/10.1061/40763(178)48.

CHENG C-L, SHALABH & GARG G. 2014. Coefficient of determination for multiple measurement error models. J Multivar Anal 126: 137-152. https://doi.org/10.1016/j.jmva.2014.01.006.

CHOW VT. 1959. Open-channel Hydraulics. McGraw-Hill, New York, 667 p.

CHOW VT, MAIDMENT DR & MAYS LW. 1988. Applied Hydrology. McGraw-Hill Series in Water Resources and Environmental Engineering, Singapore, p. 1-572.

COSTA CEAS, BLANCO CJC & DE OLIVEIRA JÚNIOR JF. 2020. IDF curves for future climate scenarios in a locality of the Tapajós Basin, Amazon, Brazil. J Water Climate Change 11(3): 760-770. https://doi.org/10.2166/wcc.2019.202.

COSTA CEAS, BLANCO CJC & DE OLIVEIRA JÚNIOR JF. 2021. Impact of climate change in the flow regimes of the Upper and Middle Amazon River. Climatic Change 166(45): 1-22. https://doi.org/10.1007/s10584-021-03141-w.

DA SILVA CRUZ J, BLANCO CJC & DE OLIVEIRA JÚNIOR JF. 2022. Modeling of land use and land cover change dynamics for future projection of the Amazon number curve. Sci Total Environ 811: 152348. https://doi.org/10.1016/j.scitotenv.2021.152348.

DUAN Y, WILSON AM & BARROS AP. 2015. Scoping a field experiment: Error diagnostics of TRMM precipitation radar estimates in complex terrain as a basis for IPHEx2014. Hydrol Earth Syst Sci 19: 1501-1520. https://doi.org/10.5194/hess-19-1501-2015.

GALINA V, CARGNELUTTI J, KAVISKI E GRAMANI LM & LOBEIRO A. M. 2018. Application of lattice Boltzmann method for surface runoff in watershed. Int J Numer Methods Calc Design Eng (RIMNI) 34(1): 10. https://doi.org/10.23967/j.rimni.2017.6.001

GEBREMICAEL TG, MOHAMED YA & ZAAG PVD. 2019. Evaluation of multiple satellite rainfall products over the rugged topography of the Tekeze-Atbara basin in Ethiopia. Int J Remote Sens 40(11): 4326-4345. https://doi.org/10.1080/01431161.2018.1562585.

GOODRICH DC, BURNS IS, UNKRICH CL, SEMMENS DJ, GUERTIN DP, HERNANDEZ M, YATHEENDRADAS S, KENNEDY JR & LEVICK LR. 2012. KINEROS2/AGWA: model use, calibration and validation. Transactions of the ASABE 55(4): 1561-1574. https://doi.org/10.13031/2013.42264.

HANTUSH MM & KALIN L. 2005. Uncertainty and sensitivity analysis of runoff and sediment yield in a small agricultural watershed with KINEROS2. Hydrol Sci J 50(6): 1150-1171. https://doi.org/10.1623/hysj.2005.50.6.1151.

HARCHE SE, CHIKHAOUI M, NAIMI M, CHOUKRI F & CHAAOU A. 2021. Comparative analysis between KINEROS2 and SWAT for hydrological modeling: A case study from Tleta Watershed in Morocco. International J Environ Agric Biotechnol 6(1): 270-281. https://doi.org/10.22161/ijeab.

HASTINGS WK. 1970. Monte Carlo sampling methods using Markov Chains and their applications. Biometrika 57(1): 97-109. https://doi.org/10.1093/biomet/57.1.97.

HUFF FA. 1967. The distribution of rainfall in heavy storms. Water Resources Research 3: 1007-1019. https://doi.org/10.1029/WR003i004p01007.

ISMAIL A, KARIM F, ROY G & MEAH MA. 2007. Numerical modelling of tsunami via the method of lines. WASET 32: 177-185.

KAIPIO JP & SOMERSALO E. 2006. Statistical and computational inverse problems. Springer Science & Business Media.

KAUTZ MA, HOLIFIELD CD, GUERTIN DP, GOODRICH DC, VAN WJ & WILLIAMS CJ. 2019. Hydrologic model parameterization using dynamic Landsat-based vegetative estimates within a semiarid grassland. J Hydrol 575: 1073-1086. https://doi.org/10.1016/j.jhydrol.2019.05.044.

KENNEDY JR, GOODRICH DC & UNKRICH CL. 2013. Using the KINEROS2 Modeling Framework to Evaluate the Increase in Storm Runoff from Residential Development in a Semiarid Environment. J Hydrol Eng 18(6): 698-706. https://doi.org/10.1061/(asce)he.1943-5584.0000655.

KIM K, WHELAN G, PURUCKER T, BOHRMANN TF, CYTERSKI MJ, MOLINA M, GU Y, PACHEPSKY Y, GUBER A & FRANKLIN DR. 2014. Rainfall-runoff model parameter estimation and uncertainty evaluation on small plots. Hydrol Proc 28: 5220-5235. https://doi.org/10.1002/hyp.10001.

KORGAONKAR Y, MELES MB, GUERTIN DP, GOODRICH DC & UNKRICH C. 2020. Global sensitivity analysis of KINEROS2 hydrologic model parameters representing green infrastructure using the STAR-VARS framework. Environ Model Softw 132: 104814. https://doi.org/10.1016/j.envsoft.2020.104814.

LAGADEC LR, PIERRE PP, BRAUD I, CHAZELLE B, MOULIN L, DEHOTIN J, HAUCHARD E & BREIL P. 2016. Description and evaluation of a surface runoff susceptibility mapping method. J Hydrol 541: 495-509. https://doi.org/1016/j.jhydrol.2016.05.049.

LANGE J & HAENSLER A. 2012. Runoff generation following a prolonged dry period. J Hydrol 464-465: 157-164. https://doi.org/10.1016/j.jhydrol.2012.07.010.

LIGHTHILL MJ & WHITHAM GB. 1955. On kinematic waves. I. Flood movement in long rivers. Proc. Royal Society London, Series A, 229(1178): 281-316.

LIMA SRM, BLANCO CJC, GOMIDE IS, BARBOSA AJS & GONCALVES MF. 2014. Analysis of the rainfall erosivity factor for a small catchment in the Amazonia. Eng & Tecnol 6(2): 184-191.

LU W & QIN X. 2020. Integrated framework for assessing climate change impact on extreme rainfall and the urban drainage system. Hydrol Res 51: 77-89. https://doi.org/10.2166/nh.2019.233.

MEMARIAM H, BALASUNDRAM SK, TALIB J, SUNG CTB, SOOD AM, ABBASPOUR KC & HAGHIZADEH A. 2012. Hydrologic Analysis of a Tropical Watershed using KINEROS2. Environment Asia 5(1): 84-93.

MICHAUD JD & SOROOSHIAN S. 1994. Effect of rainfall sampling errors on simulations of desert flash floods. Water Resources Research 30(10): 2765-2775. https://doi.org/10.1029/94WR01273.

MILLEDGE DG, LANE SN, HEATHWAITE AL & REANEY SM. 2012. A Monte Carlo approach to the inverse problem of diffuse pollution risk in agricultural catchments. Sci Total Environ 433: 434-449. https://doi.org/10.1016/j.scitotenv.2012.06.047.

MIRZAEI M, FAGHIH M, YING TP, EL-SHAFIE A, HUANG F & LEE J. 2016. Application of a rainfall-runoff model for regional-scale flood inundation mapping for the Langat River Basin. Water Practice & Technol 11(2): 373-383. https://doi.org/10.2166/wpt.2016.044.

MORAES CORDEIRO AL & BLANCO CJC. 2021. Assessment of satellite products for filling rainfall data gaps in the Amazon region. Natural Res Model 34. https://doi.org/10.1111/nrm.12298.

MOURA CHR, VIEGAS BM, TAVARES MRM, MACÊDO EN, ESTUMANO DC & QUARESMA JNN. 2021. Parameter Estimation in Population Balance through Bayesian Technique Markov Chain Monte Carlo. J Appl Comput Mech 7(2): 890-901. https://doi.org/10.22055/JACM.2021.35741.2725.

MOURA CH, VIEGAS BM, TAVARES M, MACEDO E & ESTUMANO DC. 2022. Estimation of Parameters and Selection of Models Applied to Population Balance Dynamics Via Approximate Bayesian Computational. J Heat Mass Transf Res 9(1): 53-64. https://doi.org/10.22075/JHMTR.2022.25186.1361.

NASH JE & SUTCLIFFE JV. 1970. River Flow forecasting through conceptual models' part I – A discussion of principles. J Hydrol 10(3): 282-290. https://doi.org/10.1016/0022-1694(70)90255-6.

NGUYEN HQ, DEGENER J & KAPPAS M. 2015. Flash Flood prediction by coupling KINEROS2 and HEC-RAS Models for Tropical Regions of Northern Vietnam. J Hydrol 2015(2): 242-265. https://doi.org/10.3390/hydrology2040242

NUNES KGP, DÁVILA IVJ, AMADOR ICB, ESTUMANO DC & FÉRIS LA. 2021. Evaluation of zinc adsorption through batch and continuous scale applying Bayesian technique for estimate parameters and select model. J Environ Sci Health Part A 56(11): 1228-1242. https://doi.org/10.1080/10934529.2021.1977059.

NUNES KGP, DAVILA IVJ, ARNOLD D, MOURA CHR, ESTUMANO DC & FÉRIS LA. 2022. Kinetics and Thermodynamic Study of Laponite Application in Caffeine Removal by Adsorption. Environ Proc 9(3): 1-17. https://doi.org/10.1007/s40710-022-00598-4.

OLIVEIRA RF, NUNES KGP, JURADO IV, AMADOR CB, ESTUMANO DC & FÉRIS LA. 2020. Cr (VI) adsorption in batch and continuous scale: A mathematical and experimental approach for operational parameters prediction. Environ Technol Innov: 20(2020): 101092. https://doi.org/10.1016/j.eti.2020.101092.

OSSA-MORENO J, KEIR G, MCINTYRE N, CAMELETTI M & RIVERA D. 2019. Comparison of approaches to interpolating climate observations in steep terrain with low-density gauging networks. Hydrol Earth Sys Sci 23 4763-4781. https://doi.org/10.5194/hess-23-4763-2019.

OYMAK O & SELÇUK N. 1996. Method of Lines Solution of Time-Dependent Two-Dimensional Navier-Stokes Equations. Int J Numer Methods Fluids 23(5): 455-466. https://doi.org/10.1002/(sici)1097-0363(19960915)23:5<455::aid-fld435>3.0.co;2-j.

ROMANOV AV. 2009. Inverse problem in mathematical modelling of flood waves routing. Russ Meteorol Hydrol 34: 549-555. https://doi.org/10.3103/S106837390908010X.

ROKNUJJAMAN M & ASADUZZAMAN M. 2018. On the Solution Procedure of Partial Differential Equation (PDE) with the Method of Lines (MOL) Using Crank -Nicholson Method (CNM). Am J Appl Math 6(1): 1-7. https://doi.org/10.11648/j.ajam.20180601.11.

SADIKU MNO & GARCÍA RC. 2000. Method of Lines Solution of Axisymmetric Problem. IEEE SoutheastCon 2000 Proceedings. "Preparing for The New Millennium" (Cat. No.00CH37105): 527-530. https://doi.org/10.1109/segundo.2000.845626.

SANSO B & GUENNI L. 2000. A Nonstationary Multisite Model for Rainfall. J Am Stat Assoc 95(452): 1089-1100. https://doi.org/10.2307/2669745.

SCHIESSER W & GRIFFITHS G. 2014. Method of lines solutions for the three-wave model of Brillouin equations. Engineering Computations: Int J Computer-Aided Eng Softw 31(3): 388-405. https://doi.org/10.1108/EC-05-2012-0096.

SHAKERI F & DEHGHAN M. 2008. The method of lines for solution of the one-dimensional wave equation subject to an integral conservation condition. Comput Math Appl 56: 2175-2188. https://doi.org/10.1016/j.camwa.2008.03.055.

SILVA RS, BLANCO CJC, CAVALCANTE ICS, TEIXEIRA LCGM, FERNANDES LL & PESSOA FCL. 2020. Relationship between water quality parameters and land use of a small Amazonian catchment. Sust Water Res Manag. 6(65): 1-9. https://doi.org/10.1007/s40899-020-00421-8.

SINGH VP. 1983. Analytical solutions of kinematic equations for erosion on a plane – I. Rainfall of indefinite duration. Adv Water Res (6): 2-10.

SMITH RE, GOODRICH DC, WOOLHISER DA & UNKRICH CL. 1995. KINEROS: a kinematic runoff and erosion model. In: Singh VJ (Ed), Computer Models of Watershed Hydrology. Water Resources Research. Highlands Ranch: Water Resources Publications, v. 20, p. 697-732.

SOITO JLS & FREITAS MAV. 2011. Amazon and the expansion of hydropower in Brazil: vulnerability, impacts and possibilities for adaptation to global climate change. Renew Sust Energ Rev 15(6): 3165-3177.

SORRIBAS MV, PAIVA RCD, MELACK JM, BRAVO JM, JONES C, CARVALHO L, BEIGHLEY E, FORSBERG B & COSTA MH. 2016. Projections of climate change effects on discharge and inundation in the Amazon basin. Clim Chang 136(3-4): 555-570. https://doi.org/10.1007/s10584-016-1640-2.

TOTO EA, ZOUHRI L & JGOUNNI A. 2009. Modélisation directe et inverse de l'écoulement souterrain dans les milieux poreux. Hydrol Sci J 54: 327-337. https://doi.org/10.1623/hysj.54.2.327.

VIEGAS BM, MAGALHÃES EM, ORLANDE HRB, ESTUMANO DC & MACEDO EN. 2022. Experimental study and mathematical modelling of red mud leaching: application of Bayesian techniques. International J Environ Sci Technol: 1-14. https://doi.org/10.1007/s13762-022-04346-x.

VILLARREAL ML, NORMAN LM, YAO EH & CONRAD CR. 2022. Wildfire probability models calibrated using past human and lightning ignition patterns can inform mitigation of post-fire hydrological hazards. Geom Nat Haz Risk 13(1): 568-590. https://doi.org/10.1080/19475705.2022.2039787.

WALKER WR & HUMPHERYS AS. 1983. Kinematic wave Furrow Irrigation Model. Journal of Irrigation and Drainage Engineering. ASCE, New York, 109(4): 377-392.

WOOLHISER DA & GOODRICH DC. 1988. Effect of storm rainfall intensity patterns on surface runoff. J Hydrol Eng 5(4): 355-362.

WOOLHISER DA, SMITH RE & GOODRICH DC. 1990. KINEROS, A Kinematic Runoff and Erosion Model: Documentation and User Manual. US Department of Agriculture, Agricultural Research Service, ARS-77.

How to cite
FALCÓN CT, BLANCO CJC & ESTUMANO DC. 2024. Parameter Estimation Using the Inverse Problem Method for Simulating Lateral Inflow and Runoff Depth in a small catchment of Amazon. An Acad Bras Cienc 96: e20230570. DOI 10.1590/0001-3765202420230570.

Manuscript received on May 23, 2023;
accepted for publication on October 2, 2023

CINDY T. FALCÓN[1]
https://orcid.org/0000-0001-8022-2647

CLAUDIO JOSÉ C. BLANCO[2]
https://orcid.org/0000-0003-4062-5294

DIEGO C. ESTUMANO[3]
https://orcid.org/0000-0003-4318-4455

[1]Federal University of Pará, Engineering of Natural Resources of the Amazon Graduate Program, Rua Augusto Correa, 01, Guamá, 66075-110 Belém, PA, Brazil

[2]Federal University of Pará – FAESA/ITEC/UFPA, School of Environmental and Sanitary Engineering, Rua Augusto Correa, 01, Guamá, 66075-110 Belém, PA, Brazil

[3]Federal University of Pará, School of Biotechnology and Bioprocess Engineering, Rua Augusto Correa, 01, Guamá, 66075-110 Belém, PA, Brazil

Correspondence to: **Claudio José Cavalcante Blanco**
E-mail: blanco@ufpa.br

Author contributions

Cindy Torres was responsible for conceptualization, methodology, investigation, and writing the original draft. Claudio Blanco was responsible for investigation, methodology, and review and editing. Diego Estumano was responsible for investigation, methodology, review and editing, to which all authors contributed equally.